Solution structure of native and recombinant expressed toxin CssII from the venom of the scorpion Centruroides suffusus suffusus, and their effects on Nav1.5 Sodium channels

ARTICLE *in* BIOCHIMICA ET BIOPHYSICA ACTA · MARCH 2012

Impact Factor: 4.66 · DOI: 10.1016/j.bbapap.2012.01.003 · Source: PubMed

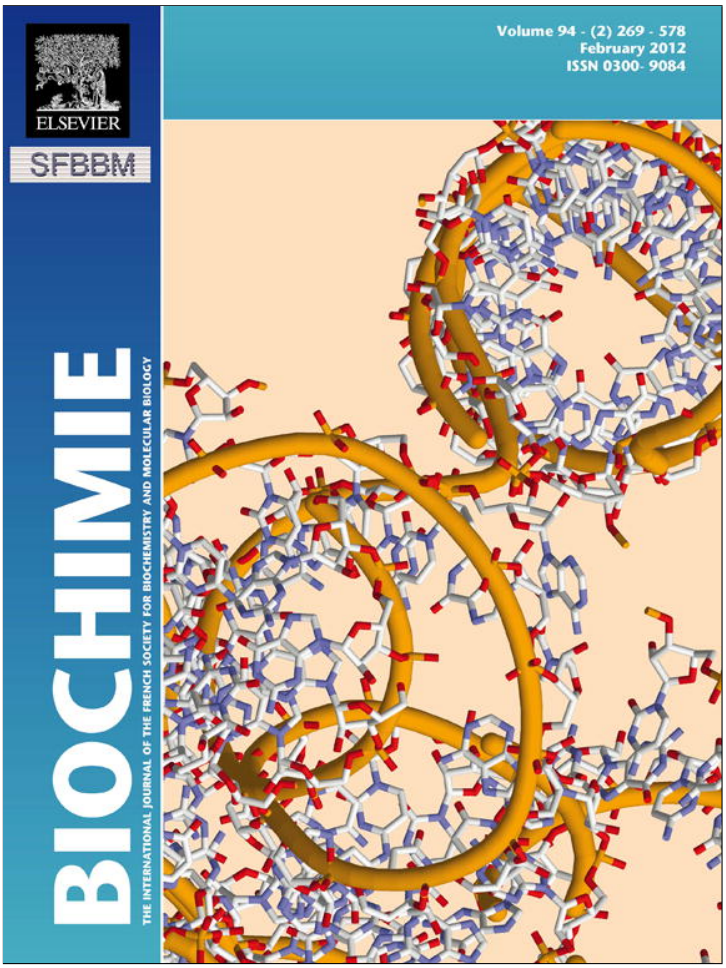

Biochimie 94 (2012) 461–470

Contents lists available at SciVerse ScienceDirect

Biochimie

journal homepage: www.elsevier.com/locate/biochi

Research paper

Pharmacological and structural characterization of long-sarafotoxins, a new family of endothelin-like peptides: Role of the C-terminus extension

Gilles Mourier[a], Mariana Hajj[b], Florence Cordier[c], Adelajda Zorba[c], XingHuang Gao[a], Tolga Coskun[b], Amaury Herbet[b], Elodie Marcon[a], Fabrice Beau[a], Muriel Delepierre[c], Frédéric Ducancel[b,*], Denis Servent[a]

[a] CEA, iBiTec-S, Service d'Ingénierie Moléculaire des Protéines (SIMOPRO), CEA Saclay, F-91191 Gif sur Yvette, France
[b] CEA, iBiTec-S, Service de Pharmacologie et d'Immnoanalyse (SPI), CEA Saclay, F-91191 Gif sur Yvette, France
[c] Institut Pasteur, Unité de RMN des Biomolécules, CNRS URA 2185, 25 rue du Dr. Roux, 75724, Paris Cedex 15, France

ARTICLE INFO

Article history:
Received 7 June 2011
Accepted 23 August 2011
Available online 29 August 2011

Keywords:
Sarafotoxins
Endothelins
Endothelin-receptors
NMR
Pharmacological profile

ABSTRACT

Long-sarafotoxins (l-SRTXs) have recently been identified in both the venom of *Atractaspis microlepidota* and that of *Atractaspis irregularis*. They are characterized by different C-terminus extensions that follow the invariant Trp21, which plays a crucial role in endothelin-receptor binding. We initially determined the toxicity and three-dimensional structures of two chemically synthesized l-SRTXs that have different C-terminus extensions, namely SRTX-m (24 aa, including extension "D-E-P") and SRTX-i3 (25 aa, including extension "V-N-R-N"). Both peptides were shown to be highly toxic in mice and displayed the cysteine-stabilized α-helical motif that characterizes endothelins and short-SRTXs, to which a longer C-terminus with variable flexibility is added. To discern the functional and pharmacological consequences of the supplementary amino acids, different chimerical as well as truncated forms of SRTX were designed and synthesized. Thus, we either removed the extra-C-terminal residues of SRTX-m or i3, or grafted the latter onto the C-terminal extremity of a short-SRTX (s-SRTX) (ie. SRTX-b). Our competitive binding assays where SRTXs competed for iodinated endothelin-1 binding to cloned ET_A and ET_B receptor subtypes over-expressed in CHO cells, revealed the essential role of the C-terminus extensions for ET-receptor recognition. Indeed, l-SRTXs displayed an affinity three to four orders of magnitude lower as compared to SRTX-b for the two receptor subtypes. Moreover, grafting the C-terminus extension to SRTX-b induced a drastic decrease in affinity, while its removal (truncated l-SRTXs) yielded an affinity for ET-receptors similar to that of s-SRTXs. Furthermore, we established by intracellular Ca^{2+} measurements that l-SRTXs, as well as s-SRTXs, display agonistic activities. We thus confirmed in these functional assays the major difference in potency for these two SRTX families as well as the crucial role of the C-terminus extension in their various pharmacological profiles. Finally, one of the chimeric toxin synthesized in this study appears to be one of the most potent and selective ligand of the ET_B receptor known to date.

1. Introduction

Snake venom sarafotoxins (SRTXs) and vertebrate endothelins (ETs) form a structurally and functionally related family of potent vasoconstrictor compounds that act on the vascular system *via* identical ET_A or ET_B receptors and modulate the contraction of cardiac and smooth muscle in different tissues [1]. This similarity is remarkable, since ETs are endogenous hormones of the mammalian vascular system while SRTXs are highly toxic components solely and highly expressed in the venom glands of snakes of the genus *Atractaspis* of the Atractaspididae family. On the other hand, ETs are autocrine or paracrine factors produced in picomolar levels in vertebrate blood by endothelial as well as other cells [2]. Classically, these peptides contain 21 amino acids and two conserved disulfide bridges between cysteines +1/+15 and +3/+11, which constitute a typical and unique Cys_1–X–Cys_3…Cys_{11}–X–X–X–Cys_{15} "signature" among bioactive peptides. They display about 60% of sequence identity, with more variable N-terminus extremities [3]. NMR and molecular modelling of the 3D structures of ET-1 [4], and SRTX-b [5] in solution demonstrate that sarafotoxins and endothelins adopt identical cysteine-stabilized α-helical motif characterized by: a) an extended structure of the four N-terminal amino acids, b) a bend between positions +5 and +8, c) an α-helical conformation of the Lys_9–Cys_{15} segment and, d) an absence of conformation of the C-terminal domain.

* Corresponding author. Tel.: +33 1 690 88154; fax: +33 1 690 89071.
E-mail address: frederic.ducancel@cea.fr (F. Ducancel).

0300-9084/$ – see front matter © 2011 Elsevier Masson SAS. All rights reserved.
doi:10.1016/j.biochi.2011.08.014

However, new bioactive 31-amino acid endothelins (long-endothelins) have been characterized in porcine lung [6]. Similarly, a new group of SRTXs called "long-sarafotoxins" (l-SRTXs) was described in *Atractaspis microlepidota microlepidota* [7] and *Atractaspis irregularis* [8]. Instead of the 10 extra amino acids found in long-endothelins ET-1(1–31), the C-terminus extremities of l-SRTXs display various length and amino acid composition with which some C-termini being identical or similar to the tails that ends ET-1(1–31) [9]. In particular, a study on SRTX-m, a long-sarafotoxin from *A. microlepidota microlepidota*, revealed: i) a high toxicity in mouse, ii) a vasoconstriction activity and most surprisingly iii) a failure to displace binding of labelled SRTX-b together with an absence of direct binding to atrial membrane preparations [7]. Together, these results suggest that l-SRTXs might form a distinct group within the endothelin-like family, group in which the additional C-terminal residues could confer original binding and pharmacological properties.

To assess this hypothesis, we have explored in this article the structural, functional and pharmacological consequences of the C-terminus extensions that characterize l-SRTXs. To reach that goal, we chemically synthesized different natural and C-terminus engineered SRTX isoforms: i) natural long-sarafotoxins SRTX-m and SRTX-i3 that respectively display "D-E-P" or "V-N-R-N" extensions, ii) truncated 21 amino acids long-STRX-m and SRTX-i3 from which we removed the additional C-terminal residues, and iii) engineered long-SRTX-b, corresponding to the native short-SRTX-b onto which we grafted "D-E-P" or "V-N-R-N" originating respectively from the C-terminal extremities of SRTX-m or SRTX-i3. We show here that NMR structures of SRTX-m and SRTX-i3 are similar to those of endothelins and s-SRTXs previously reported with however more or less restricted conformations of their long C-terminal tail. Using cloned and CHO over-expressed ET_A and ET_B receptors, we demonstrate that i) l-SRTXs as well as s-SRTXs interact more efficiently on ET_B as compared to ET_A receptors, ii) the presence of a C-terminus extension, independently of its nature, is systematically associated with a decrease by several orders of magnitude in the affinity for both receptor subtypes, iii) and that all the SRTXs display agonistic activities with a potency that is drastically affected by the C-terminus extension as shown by intracellular Ca^{2+} measurements. Interestingly, despite very low *in vitro* affinity constants for both ET-receptors, l-SRTXs display LD_{50} values in mouse just slightly higher than those of s-SRTXs. This observation raises the question about the way by which l-SRTX might express their toxicity *in vivo*, for example *via* a specific proteolytic maturation, *via* an interaction with an atypical ET-receptor subtype or by activating multiple signalling pathways.

2. Materials and methods

2.1. Materials

[^{125}I]-Endothelin-1, (2200 Ci/mmol) was from PerkinElmer (Courtaboeuf, France) and cold Endothelin-1 and SRTX-b from Sigma (St Quentin Fallavier, France). Automated chain assembly was performed on a standard Applied Biosystems 433 peptide synthesizer (Applied Biosystems, France).

2.2. Peptide synthesis, disulfide bond formation and protein purification

The different sarafotoxins and their analogues were synthesized on a Fmoc-Trp(Boc)-wang resin, or a Fmoc-Asn(Trt)-wang resin or a H-Pro-2ClTrt-resin (Novabiochem) by standard solid phase synthesis techniques utilizing the Fmoc strategy previously described for the synthesis of the muscarinic toxins [10]. Dicyclohexylcarbidiimide/6-Chloro-1-hydroxybenzotriazole were used as coupling reagents. All the cysteines were introduced as Fmoc-Cys(Trt)-OH. The peptides were cleaved from the resin after the TFA deprotection step, and for each peptide the crude material was purified by HPLC using a C18 column with a gradient of 18–30% CH_3CN in 0.1%TFA in water in 40 min. The reduced form of each peptide was subjected to an oxidative reaction in 0.1 M Tris, 1 mM EDTA buffer (pH 8) containing 0.5–2 M guanidine hydrochloride in the presence of reduced (GSH) and oxidized (GSSG) glutathione in a molar ratio of 1/10/100 in peptide/GSSG/GSH at a peptide concentration of 0.05 mg/ml as described elsewhere [10]. After 24–36 h at 4 °C the oxidized forms of the toxins were purified to homogeneity by HPLC and characterized by amino acid analysis using an Applied Biosystems model 130A automatic analyzer and mass spectrometry on a Nermag spectrometer coupled to an analytical (Brandford) electrospray source. The concentrations of the different toxins were evaluated by spectrometry approaches.

2.3. NMR structure characterization

2.3.1. Sample preparation for NMR measurements

NMR samples (3 mm Shigemi NMR tubes) of the two peptides SRTX-m and SRTX-i3 were prepared by dissolving 0.7 mg (1.4 mg) of lyophilized SRTX-m (SRTX-i3), in 160 µl of 88% H_2O/12% D_2O, leading to a concentration of 1.5 mM (3 mM) at pH 5 (pH 4.5).

2.3.2. NMR spectroscopy and structure calculation

Standard 2D homonuclear ^{1}H experiments were carried out on a Varian Inova 500 MHz spectrometer and a 600 MHz spectrometer equipped with a cryoprobe. Purged-COSY (recorded at 25 °C on SRTX-m and SRTX-i3 samples), TOCSY (15, 25 and 35 °C on SRTX-m and SRTX-i3 samples; mixing time $\tau_m = 80$ or 100 ms) and NOESY (25 °C for SRTX-m and 25 and 35 °C for SRTX-i3 sample; $\tau_m = 250$ ms) experiments were acquired for proton resonance assignment and ^{1}H–^{1}H NOE restraints. Data acquisition, processing and analysis were performed as previously described [11]. Chemical shifts were referenced relative to the sodium salt of 4,4-dimethyl-4-silapentane sulfonate. Proton resonance assignments were achieved by the standard homonuclear method [12]. Structures of SRTX-m and SRTX-i3 were calculated with the program ARIA1.2 (Ambiguous Restraints for Interactive Assignment) [13] as an extension of CNS 1.1 [14], from NMR data obtained at 25 °C (SRTX-m) and 25 and 35 °C (SRTX-i3). After refinement in an explicit water box [13], the 10 refined conformers of lowest energy were selected to represent the final NMR ensemble and were analyzed with PROCHECK 3.54 [15]. More details on structure calculations are given in the Supplementary data. The statistics of the ensembles and of the experimental restraints are given in Supplementary data Table S1.

The coordinates and structural restraints have been deposited in the Brookhaven Protein Data Bank under accession code 2LDFfor SRTX-m and 2LDE for SRTX-i3.

2.4. Sarafotoxins in vivo toxicity

Animals use procedures were in accordance with recommendations of the EEC (86/609/CEE) and the French National Committee (decree 86/848) for the care and use of laboratory animals.

Eight-weeks-old male balb-C mice (Charles Rivers Laboratories, Les Oncins, France) weighting from 20 to 25 g were used in these experiments. Mice were placed in polycarbonate cages (10 in each cage) at a controlled room temperature of 22 ± 2 °C, with a relative humidity from 30 to 70% and a constant light–dark schedule (12 h light and 12 h dark cycle). Animals were fed with control-certified

diets A03 supplied by SAFE (France) and fresh water *ad libitum*. All animals were acclimatized to laboratory condition for a week before the beginning of the experiment.

Animals were divided into four groups of 10 animals. Group I was treated with the vehicle (physiological serum – 0.15 M NaCl) and was kept as negative control. Groups II, III and IV were treated with sarafotoxin-i3 at the doses of 150, 30 and 3 ng/g of body weight corresponding to high, intermediate and low doses. Sarafotoxin-i3 was administered within a single intravenous injection of each formulation into the tail vein of mice. Animals were beforehand anesthetised with isoflurane (2%). LD_{50} of sarafotoxin-i3 was estimated by scoring death within 24 h following injection of 0.1 ml of the tested peptide in 0.15 M NaCl. Animals were observed during the first hours.

2.5. ET-CHO cells and membrane preparation

Dr. Sabrina Corrazza (AxxamSpA, Milan, Italy) kindly provided CHO cells stably expressing the human ET_A receptors. For ET_B, a stable cell line was obtained after transfection or CHO cells with the cDNA coding for the human ET_B receptor and classical selection process with neomycin resistance (G418).

The cells were grown in plastic Petri dishes (Falcon) which were incubated at 37 °C in an atmosphere of 5% CO_2 and 95% humidified air in Ham F12 medium pre-complemented with L-glutamine and bicarbonate (Sigma) supplemented with 10% foetal calf serum and 1%penicillin/streptomycin (Sigma). At 100% confluence, the medium was removed and the cells were harvested using Versen buffer (PBS + 5 mM EDTA). They were washed with ice-cold phosphate buffer and centrifuged at 1700 g for 10 min (4 °C). The pellet was suspended in ice-cold buffer (1 mM EDTA, 25 mM Na phosphate, 5 mM $MgCl_2$, pH 7.4) and homogenized using an Elvehjem-Potter homogenizer (Fisher Scientific Labosi, Elancourt, France). The homogenate was centrifuged at 1700 g for 15 min (4 °C). The sediment was resuspended in buffer, homogenized and centrifuged at 1700 g for 15 min (4 °C). The combined supernatants were centrifuged at 35,000 g for 30 min (4 °C) and the pellet was suspended in the same buffer (0.1 ml/dish). Protein concentrations were determined according to the Lowry method using bovine serum albumin as standard. The membrane preparations were aliquoted and stored at −80 °C.

2.6. Equilibrium [^{125}I]-Endothelin-1 binding assays

The effect of ET-1 and SRTXs on the equilibrium binding of [^{125}I]-Endothelin-1 for ET_A and ET_B receptors was determined with equilibrium inhibition binding experiments. Membrane protein concentrations, adjusted so no more than 10% of added radioligand was specifically bound (around 1500–2000 cpm), were incubated in PBS–BSA at 25 °C for at least 2 h, with varying concentrations of ligand and [^{125}I]-Endothelin-1 (25–50 pM), in a final assay volume of 200 μl. Non-specific binding was determined in the presence of 0.1 μM ET-1. The reaction was stopped by addition of 3 ml of ice-cold buffer (PBS) immediately followed by filtration through Whatman GF/C glass fibre filters pre-soaked in 0.5% polyethylenimine. The filters were washed once again with 3 ml ice-cold buffer (PBS), and the bound radioactivity was counted in a gamma counter (LKB 1261 multigamma). Each experiment was done at least three times in duplicate. The binding data from individual experiments were analyzed by nonlinear regression analysis using Kaleidagraph 4.0 (Synergy Software, Reading, PA) and the IC_{50} values were converted to Ki constants using the following equation: $Ki = IC_{50}/(1 + L^*/Kd)$ [16], with a Kd [^{125}I]-Endothelin-1 for ET_A and ET_B receptors equal to 46 pM and 25 pM, respectively [17].

2.7. Intracellular calcium assays

CHO cells stably expressing ET_A and ET_B receptors were plated (30,000–50,000 cells/well in100 μl) on black-walled 96-well plates (Greiner). 24 h after coating, the cells were incubated 45 min with the no-wash CaKit dye resuspended in Hank Balanced Salt Solution (HBSS) buffer complemented with Hepes 20 mM, at pH 7.4 (R8041, Molecular Devices Ltd, Wokingham, UK). The fluorescence was recorded using a FlexStation II plate reader (Molecular Devices Ltd, Wokingham, UK) with an excitation and emission wavelengths fixed at 485 and 525 nm, respectively. Drug dilutions in assay buffer were prepared in a separate 96-well plate. Parameters for drug addition to the cell plate were preprogrammed and delivery of the agonist ET-1 or sarafotoxins was automated through a 8-tip head pipettor, 20 s after the beginning of the recording. Dose-response curves were constructed by measuring the fluorescence intensity after normalization to the maximal response to ET-1. All data points were measured at least three times in duplicate.

3. Results

3.1. Design and chemical synthesis of wild-type and modified sarafotoxins

All the different analogues of SRTXs corresponding to the native sequences, the truncated SRTX-m and SRTX-i3 to which additional C-terminal residues were removed and also two peptides corresponding to the native SRTX-b onto which the "D-E-P" or "V-N-R-N" tail were grafted. The progress of the assembly was monitored by UV detection of the dibenzofulvene adduct from the Fmoc deprotection. The step by step assembly of the peptide chain proceeded smoothly and all the amino acids were fully incorporated after a single coupling. After the final TFA deprotection step, all the synthetic peptides corresponding to the reduced forms of the different SRTX analogues and containing the four free sulfhydryls were refolded *in vitro*. The complete disulfide formation was achieved in presence of reduced and oxidized glutathione and guanidine to minimize the formation of aggregates often observed during the refolding process [18]. As shown on Fig. 2A, the refolding of the native or truncated SRTX-m (data not shown) results in a mixture of two different forms present in a ratio of 3:1. The major component that displays higher retention time corresponds to the native cysteine pairing (1–15, 3–11) when the minor form is a misfolded isomer, as it was observed during the refolding of ET-1 [19]. Interestingly, the presence of non native isomers was also observed during the refolding of the native and truncated SRTX-i3 and for the two analogues of SRTX-b but in a lower ratio and represent minor components, less than 10%, as compared to the major component corresponding to the native isomer (Fig. 2B). All the major

```
ET1.....................  CSCSSLMDKECVYFCHLDIIW
                          1        10        20
Sft c                     CTCNDMTDEECLNFCHQDVIW
Sft b...................  CSCKDMTDKECLYFCHQDVIW
Sft i3..................  CSCTDMSDLECMNFCHKDVIW V N R N
Sft m...................  CSCNDINDKECMYFCHQDVIW D E P

Sft b + Ct(m) .......     CSCKDMTDKECLYFCHQDVIW D E P
Sft b + Ct (i3).....      CSCKDMTDKECLYFCHQDVIW V N R N

Sft m - Ct..............  CSCNDINDKECMYFCHQDVIW
Sft i3 - Ct.............  CSCTDMSDLECMNFCHKDVIW

Concensus...............  CSC----D-EC--FCH-D-IW
```

Fig. 1. Sequence alignment of investigated endothelins and sarafotoxins. The two conserved disulfide bridges are indicated on the ET-1 sequence and the consensus sequence indicates the residues conserved in all the peptides.

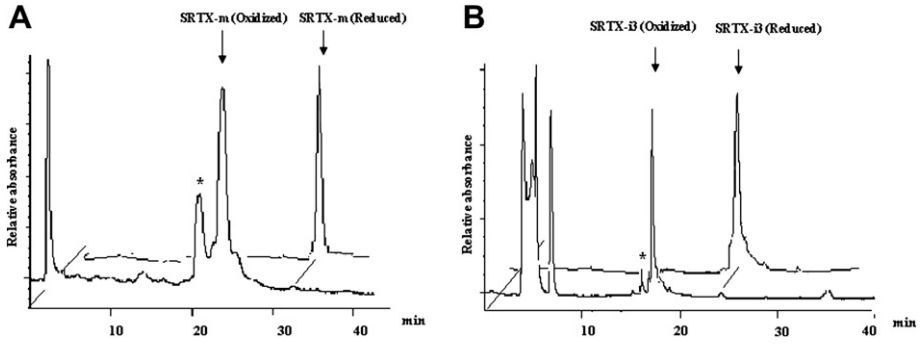

Fig. 2. Analytical HPLC profiles of the reduced form and the glutathione-mediated oxidative form of A: SRTX-m and B: SRTX-i3. The asterisk indicates the peak corresponding to the minor misfolded isomer. RP-HPLC conditions: C18 analytical column (0.45 × 15 cm) with a gradient of 18–30% CH_3CN in 0.1%TFA in water in 40 min at a flow rate of 1 ml/min. Protein detection was followed at 214 nm.

components exhibited the expected molecular masses namely 2902.9 for SRTX-m (theoretical 2902.7), 2562.4 for SRTX-m-Ct (theoretical 2562.8), 2959.7 for SRTX-i3 (theoretical 2960.3), 2476.2 for SRTX-i3-Ct (theoretical 2476.7), 2903.9 for SRTX-b+Ctm (theoretical 2903.1), 3045.9 for SRTX-b+Cti3 (theoretical 3045.3) and the expected amino acid composition. They were produced at several mg amounts and were used in the NMR structural characterizations and biological assays.

3.2. Solution structures of SRTX-m and SRTX-i3 and comparison to SRTX-b and ET-1

The structure calculations were performed as described in Materials and methods, from NMR data obtained at 25 °C (SRTX-m) and at 25 and 35 °C (SRTX-i3), and structural statistics are given in Supplementary data Table S1. Both SRTX-i3 and SRTX-m structures (Fig. 3A and B) consist of an extended region (residues 1–4), a bend (residues 5–7), an α-helix (residues 8–15) and a long C-terminus tail (residues 16–24/25).

3.2.1. The cysteine-stabilized α-helical motif

The so-called cysteine-stabilized α-helical motif (CSH), commonly found in bioactive peptides such as endothelins, sarafotoxins, bee and scorpion toxins, contains a consensus cystine framework, Cys–(X)1–Cys/Cys–(X)3–Cys, which has been found to induce and stabilize this folding motif [20]. In the case of sarafotoxins, the structure contains in addition to the extended region (residues 1–4), a bend (residues 5–7) and an alpha-helix

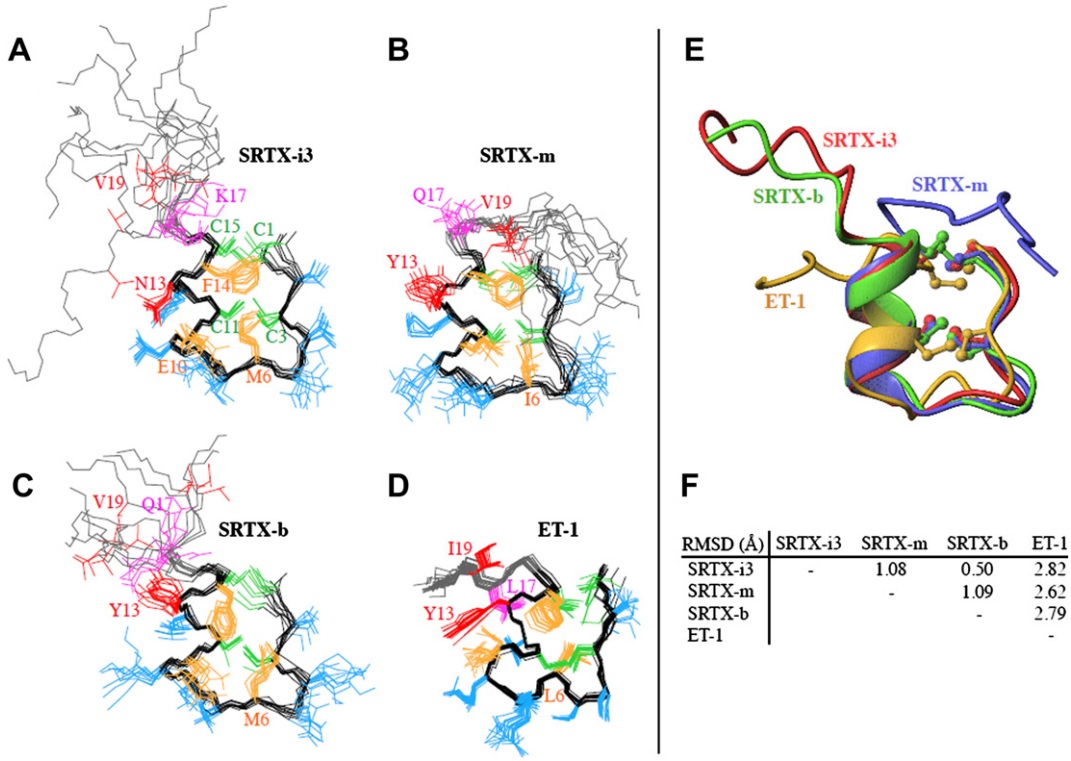

RMSD (Å)	SRTX-i3	SRTX-m	SRTX-b	ET-1
SRTX-i3	-	1.08	0.50	2.82
SRTX-m		-	1.09	2.62
SRTX-b			-	2.79
ET-1				-

Fig. 3. Solution structures of SRTX-i3 and SRTX-m and comparison to SRTX-b and ET-1. (A, B, C, D). The NMR ensembles of SRTX-i3 and SRTX-m (A and B, this work), SRTX-b (C, pdb code *1srb*, [5]) and ET-1 (D, pdb code *1v6r*, [22]) are shown in black (backbone) and blue (side chains) for the folded region C1–C15 forming the CSH motif and in grey (backbone) for the C-terminus tail. Side chains of Cys residues involved in S–S bridges are shown in green. The conserved hydrophobic M/I/L6 and F14 residues as well as the conserved E10 residue are in orange. Other residues discussed in the text are shown in red (N/Y13, V/I19) and magenta (K/Q/L17). Note that the ET-1 structure is extremely well defined since it was calculated with 32,000 initial structures (see text). (E) Superposition of a representative structure of SRTX-i3 (red), SRTX-m (blue), SRTX-b (green, pdb code *1srb*) and ET-1 (orange, pdb code *1v6r*). Side chains of Cys residues involved in S–S bridges are shown in balls and sticks. (F) Table of backbone pairwise RMSD (in Å) for residues 1–15. RMSD were calculated using the mean structures. (For interpretation of the references to colour in this figure legend, the reader is referred to the web version of this article.)

(residues 8–15), the extended region being linked to the helix by two disulfide bridges C1/C15 and C3/C11. The conserved hydrophobic residues I6/M6 and F14, as well as the aliphatic part of the strictly conserved E10 side chain are particularly well defined in the NMR ensembles and form a small stabilizing hydrophobic core. For the folded region C1-C15, both structures are rather well defined, with a root mean square deviation (RMSD) on the backbone and heavy atoms of 0.54 and 1.05 Å for SRTX-m and 0.50 and 0.83 Å for SRTX-i3. The CSH fold of SRTX-m and SRTX-i3 is also very similar to that of SRTX-b (RMSD of 1.09 and 0.50 Å) and to a lesser extent to that of ET-1 (RMSD of 2.62 and 2.82 Å) (Fig. 3E and F).

3.2.2. The long C-terminus tail

In the SRTX-i3 structure, the long C-terminus tail from H16 to N25 is found conformationally flexible and disordered, without any detectable interaction with the folded N-terminus CSH motif. This is due to the absence of NOE connectivities between these two regions and in agreement with the small dispersion of amide proton chemical shifts for residues H16 to N25 (7.8–8.3 ppm). In addition, the chemical shifts of the Hα proton corrected for random coil values (δHα-rc) are close to zero, which points towards the absence of regular secondary structure elements. Only the slight negative $_{\delta}H_{\alpha\text{-rc}}$ values (around −0.2 ppm) of the two isolated residues V22 and N23 (see Supplementary data Fig. S2) could suggest a local residual structure such as part of a helix turn within this flexible tail.

At the opposite, in SRTX-m, the conformation of the long C-terminus tail is found more restricted. Unlike for SRTX-i3, NOE connectivities are observed between the end of the α-helix (side chains of Y13 and F14) and the beginning of the C-terminus tail (side chains of Q17 and V19) (Supplementary data Fig. S1). As a result, the residues H16 to V19 are loosely looped back onto the small hydrophobic patch, restricting large amplitude motions of the C-terminus extremity.

3.2.3. Comparison to SRTX-b and ET-1 solution structures

In the SRTX-b structures, the shorter C-terminus tail (residues H16-W21) was found to be very flexible and without any regular secondary structures (Fig. 3C) [5], as in our SRTX-i3 structure. This is also the case for the ET-1 C-terminus tail, when the structure calculation was performed with a conventional number of initial structures (see Fig. 3 of [22]). However, Takashima et al. claimed that the ET-1 structures calculated with tens of thousands of initial structures (for a better sampling of the conformational space) have a well defined C-terminal conformation (Fig. 3D). In this case, a similar proximity is found between the side chains of Y13, F14, L17 and I19 as in our SRTX-m structure, although the orientation of the rest of the C-terminus differs.

3.3. Toxicity of long-sarafotoxin-i3

Doses of 3, 30 and 150 ng of SRTX-i3/g body weight were tested on three groups of ten mice and the calculated LD_{50} was in the range of 100–150 ng/g of body weight. This value is 8- to 10-times higher than the LD_{50} of the more toxic isoform SRTX-b [21] and about 4-times higher than LD_{50} value previously determined for the long-SRTX-m from *A. microlepidoda* [7]. In the control group, no death was observed, while for the lower dose (i.e. 3 ng/g body weight) alls animals survived and appeared normal. For the intermediated dose (i.e. 30 ng/g body weight), after 90 min of amorphous behaviour and a retrieval step of 4 h, all the animals survived. For the higher dose (i.e. 150 ng/g body weight), all animals have a moribund appearance post injection but only six mice died within 24 h.

3.4. Pharmacological characterization of the short, long and modified sarafotoxins

The binding affinities of ET-1, short, long and modified SRTXs to ET_A and ET_B receptors stably expressed in CHO cells were determined in a [^{125}I]-Endothelin-1 competition binding assay. First, as shown on Fig. 4, ET-1 interacts with high affinity with both receptor subtypes, with affinity constants equal to 21 pM and 150 pM on ET_A and ET_B, respectively (Table 1). At the maximal concentration tested, all the ligands studied were able to totally displace the radioactive tracer on the ET_B receptor (Fig. 4A). Two groups of ligands emerged: on one hand the highly potent molecules with picomolar affinities, including the ET-1, the SRTX-b, the SRTX-m-Ct and the SRTX-i3-Ct and on the other hand the ligands with affinities in the micromolar range which included SRTX-m, SRTX-i3, SRTX-b+Ctm and SRTX-b+Cti3 (Fig. 4A, Table 1). Thus, the presence of the C-terminal extension induces drastic 4-orders of magnitude decrease in affinity of l-SRTX for ET_B receptor. More interestingly, the simple deletion of these three/four additional residues is sufficient to convert these very low affinity ligands into picomolar binders while at the same time the addition of these extensions onto the SRTX-b induces a dramatic loss of affinity (Table 1). On the ET_A receptor (Fig. 4B), with the exception of the quasi-equipotent ET-1, all the other SRTXs interacted with lower affinities as compared to ET_B subtype, making impossible the precise determination of the affinity constants of some l-SRTXs (Fig. 4B, Table 1). Moreover, similarly to the ET_B receptor, the natural presence or the grafting of a C-terminal extension onto the SRTX sequence, whatever its nature, induced a sharp affinity decrease of SRTXs for the ET_A receptor of at least 3-orders of magnitude. Nevertheless, although the deletion of the DEP sequence from SRTX-m makes this ligand as potent as SRTX-b, it was not the case for SRTX-i3-Ct that is characterized by an intermediate affinity between l-SRTX and s-SRTX. Dealing with the ET_A/ET_B receptor selectivity, it is interesting to note that all the SRTXs studied interact preferentially with ET_B receptor but with large differences between the less selective SRTX-b+Ctm (one order of magnitude between ET_B and ET_A), the SRTX-m, SRTX-i3 and SRTX-b+Cti3 (2 orders of magnitude), the SRTX-m-Ct and SRTX-b (about 3-orders of magnitude) and finally the most selective toxins, the SRTX-i3-Ct that interacts with ET_B receptor with an affinity constant more than 10,0000-times better as compared to ET_A receptor (Table 1).

3.5. Functional characterization of the short, long and modified sarafotoxins

The agonistic effects of ET-1, wild-type and modified sarafotoxins on ET_B receptor stably expressed at the surface of CHO cells was evaluated by measuring the fluorescence of a calcium dye that varies according to the intracellular calcium concentration. First, the agonistic effect of ET-1 was highlighted by the dose-dependent release of intracellular calcium observed with increasing concentrations of ET-1, allowing the calculation of an pEC_{50} value equal to 7.91 (Fig. 5A and B, Table 2). Similarly, activation dose–response curves were measured for the different SRTXs, showing the full agonist property of wild-type and modified toxins and highlighting the high (EC_{50} in the 10 nM range) and low (EC_{50} in the micromolar range) potency of s-SRTXs (SRTX-b, SRTX-m-Ct, SRTX-i3-Ct) and l-SRTXs (SRTX-m, SRTX-b+Ctm, SRTX-b+Cti3), respectively (Fig. 5B) (Table 2). Due to its low agonist potency, the agonist efficacy of SRTX-b+Ctm cannot be determined precisely and similarly, the absence of fluorescent signal measured with micromolar concentration of SRTX-i3 do not allowed to evaluate its potency.

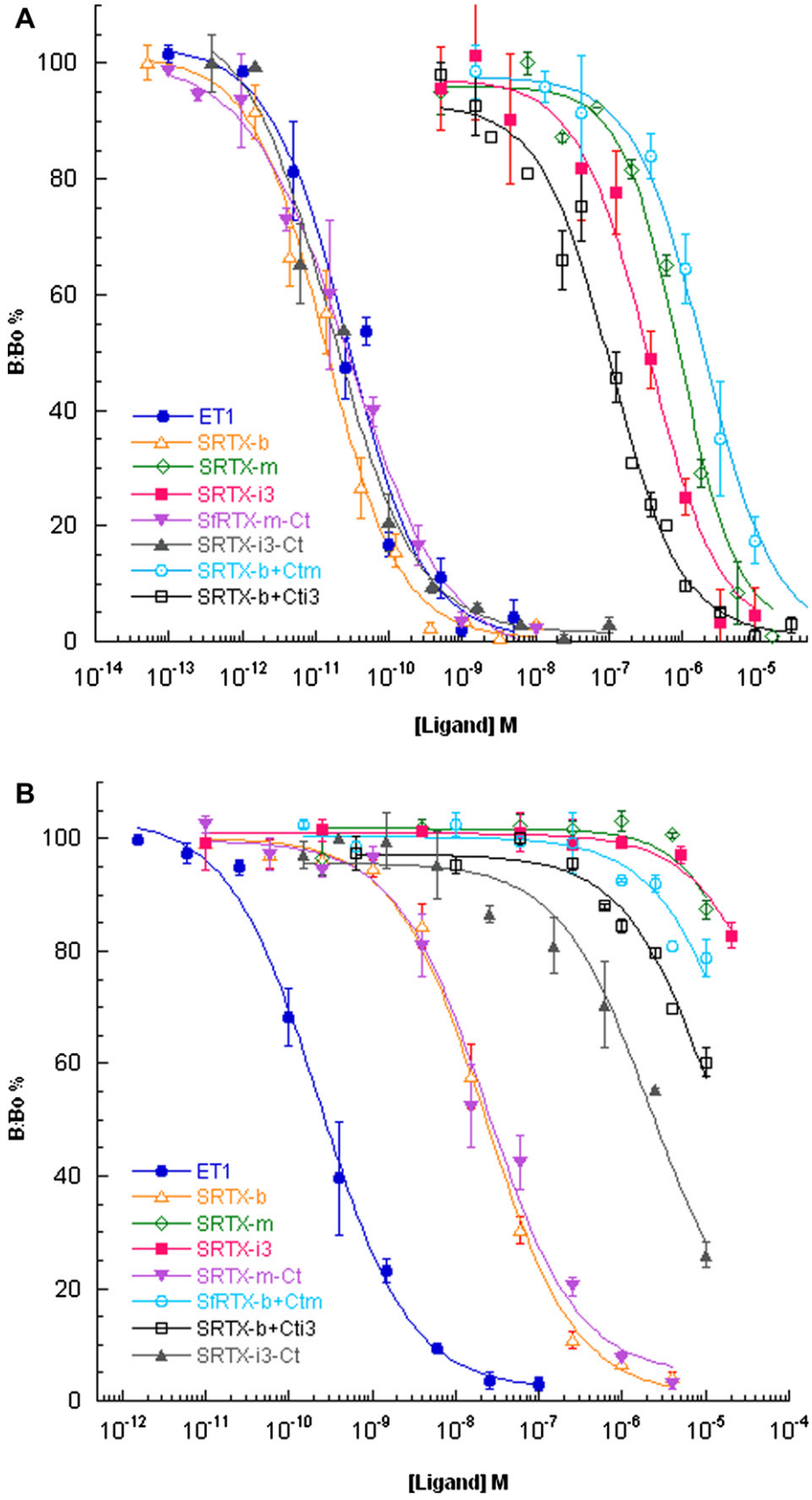

Fig. 4. Competition binding experiments of ET-1, s-SRTXs and l-SRTXs on ET_B (A) and ET_A (B) receptors. The binding curves were obtained by incubating [^{125}I]-ET-1 with increasing concentrations of ligands. The results are expressed as the ratio of the specific [^{125}I]-ET-1 binding measured with (B) or without ligands (Bo). Each value represents the mean ± SEM of three to eight experiments.

Table 1
Affinity constants of ET, s-SRTX, l-SRTXs and modified toxins on ET_A and ET_B receptors (Ki in nM).

Ligands	Ki on ET_A	Ki L/Ki SRTX-b	Ki on ET_B	Ki L/Ki SRTX-b	ET_A/ET_B
ET-1	0.15 ± 0.01	0.01	0.021 ± 0.005	1.3	7.2
ET3[a]	420	30	0.130	8	3230
SRTX-c[a,b]	14,500	1000	0.1	6.2	145,000
SRTX-b	14.1 ± 0.9	1	0.016 ± 0.007	1	875
SRTX-m	>50,000	>5000	780 ± 90	48,450	>64
SRTX-i3	>50,000	>5000	380 ± 180	23,600	>131
SRTX-b+Ctm	42,000 ± 17,000	2979	1800 ± 100	111,800	23
SRTX-b+Cti3	24,000 ± 10,700	1702	95 ± 13	5900	253
SRTX-m-Ct	14.1 ± 9.3	1	0.021 ± 0.004	1.3	681
SRTX-i3-Ct	2150 ± 250	152	0.018 ± 0.004	1.1	119,500

[a] [32].
[b] [33].

4. Discussion

Based on a combined molecular cloning of the precursors encoding SRTXs and on the MS/MS *de novo* sequencing of snake venoms, several new isoforms of SRTXs have been recently identified from Atractaspisdidae venom [7,9]. This new family of SRTXs isopeptides, called long-SRTXs, possesses a C-terminal extension after the consensus Trp21 varying from 2 to 9 residues. However, the major l-SRTXs found in these venoms, such as SRTX-m in *A. microlepidota microlepidota* or SRTX-i3 in *A. irregularis* venoms, display 3 and 4 additional C-terminal amino acids, respectively. Preliminary results on SRTX-m report on its high toxicity and vasoconstriction activity and strikingly point to the absence of binding property to atrial membrane preparations [7]. Thus, in order to identify whether the additional C-terminal residues could confer some original structural and/or pharmacological properties to l-SRTXs, various natural and modified SRTXs were chemically synthesized in order to be structurally and pharmacologically studied.

At the structural level, comparison of the NMR models previously reported for SRTX-b [5] or ET-1 [22] and those of SRTX-i3 and SRTX-m presented in this paper, highlights the strong structural conservation of the extended region (C1-X4), bend part (X5-X7) and helix structures (D8-C15), while the C-terminal extensions (H16-W21 or H16-X24/X25) diverge in flexibility and orientation. Moreover, scrutiny of the electrostatic surface potential of SRTX-b, SRTX-m and SRTX-i3 reveals that even if small differences in the location of charged residues exist, the global charged distribution is conserved between the different SRTXs (see Supplementary data Fig. S3). Indeed, the four negatively charged D5, D8, E10 and D18 are strictly conserved ensuring the acidic isoelectric point of all these SRTXs (between 4 and 4.7) while the number (one or two) and location of Lys and Arg are more variable. Thus, the similar electrostatic surface potential of SRTX-b and SRTX-i3 does not support a major role of minor variations in charged distribution in the large difference in interaction of s-SRTX and l-SRTX with ET-receptors. So, it is tempting to postulate that the bulky hindrance associated with the C-terminal extension may affect the ability of l-SRTXs to interact with their ET-receptor targets, in agreement with the highly critical role previously reported for the Trp21 residue located in this region [23,24].

First biological studies regarding the toxicity in mouse of these l-SRTXs do not seem to validate this hypothesis. Indeed, the calculated LD_{50} of SRTX-i3 (120 μg/kg) is only 8-fold higher than those of SRTX-b or ET-1 [21] and 3-times higher than the previously characterized value of SRTX-m [7]. Thus, even if the toxicity of l-SRTXs is weakly decreased as compared to s-SRTXs, the presence of the C-terminal extension does not seem to affect drastically the lethal effect of these toxins.

Interestingly, *in vitro* pharmacological characterizations of all these toxins on cloned human ET_A and ET_B receptors lead to quite different observations and highlight the major role of the C-terminal extension in the SRTXs-ET-receptors interaction. First, the two natural l-SRTXs studied in this paper interact with 3- to 4-orders of magnitude lower affinity with ET_A and ET_B as compared to s-SRTX. This observation could be compared with the decrease of affinity on ET_B receptor previously observed with the 31 amino acids-length endothelin (ET-1 1–31) [6], even if the affinity decrease was smaller than those observed with l-SRTX. More interestingly, grafting the C-terminal extension from SRTX-m (DEP) as well as SRTX-i3 (VNRN), onto the SRTX-b scaffold is sufficient to drastically decrease its affinity on both receptor subtypes to the same values as l-SRTXs (Table 1). Thus, this effect seems independent of the size and composition of the C-terminal extension and affects both receptor subtypes identically, suggesting a potential steric hindrance associated with this extension in the SRTX-ET-receptor interaction. This hypothesis is reinforced by the recovery of a high affinity pharmacological profile, such as with SRTX-b, associated with the deletion of the C-terminal extension on SRTX-m and SRTX-i3, even if the recovery was not total for SRTX-i3-Ct on ET_A receptor (Table 1). Thus, the pM and μM affinity of this last compound on ET_B and ET_A, respectively, defines this compound as one of the most potent and selective ligand of the ET_B receptor.

Furthermore, a recent study analyzing the structural determinants involved in the interaction of endothelins and SRTXs on their ET_A and ET_B receptor targets proposes that the ligand selectivity was mainly supported by the different shapes of the extracellular domains of these receptors governing the accessibility to the transmembrane binding sites [25]. In their model, the authors place the C-terminal part of endothelins or s-SRTX (H16-W21) at the centre of TM domains (TM3, TM5, TM6, TM7) that define the typical binding sites for small ligands on these receptors. More particularly, W21 is predicted to play a crucial role by interacting with its carboxyl group and indole moiety with conserved residues of ET-receptors, in agreement with its major role in ET interaction and activation properties [24,26]. Thus, the proposed location of this C-terminal region in the core of TM domains of the receptor reinforces the hypothesis of steric clashes and/or structural rearrangement of natural and engineered l-SRTXs within the binding sites associated with the addition of 3–4 residues at the C-terminal tail. Nevertheless, if the presence of this extension is highly deleterious for the affinity of the l-SRTXs on both receptor subtypes, the effect was not so drastic on their agonist potency. Indeed, measuring the Ca^{2+} release following the ET_B activation with ET-1, SRTX-b, l-SRTXs or modified SRTXs, allows to demonstrate first the full agonist property of all these ligands and also to measure a difference in potency varying between 40- to 450-fold for ET-1, SRTX-b, SRTX-m-Ct and SRTX-i3-Ct on one hand and SRTX-m, SRTX-b+Cti3 and SRTX-b+Ctm on the other hand. More precisely, the 40-fold decrease in agonist potency (pEC_{50}) of SRTX-m as compared to SRTX-b is highly similar to the difference in ED_{50} previously observed for their capacity to induce the contraction of rabbit aorta strips [7]. At the molecular level, the relatively limited effect of the C-terminus extension on the agonist potency of l-SRTX suggests that the location of the residues determining the agonist property, such as D8 and E10, would not be totally disturbed within the receptor binding site. Superimposition of the NMR structures of SRTX-m, i3 and b, showing a very low RMSD for residues 1–15 (0.5–1 Å) (Fig. 3), reinforces this hypothesis. Nevertheless, the perturbation of the interaction between W21 on the l-SRTXs and W6.48 (Ballesteros–Weinstein numbering) on the receptor, that participate to the agonist/antagonist switch [19,25,27], may account for the decrease in agonist potency of these ligands.

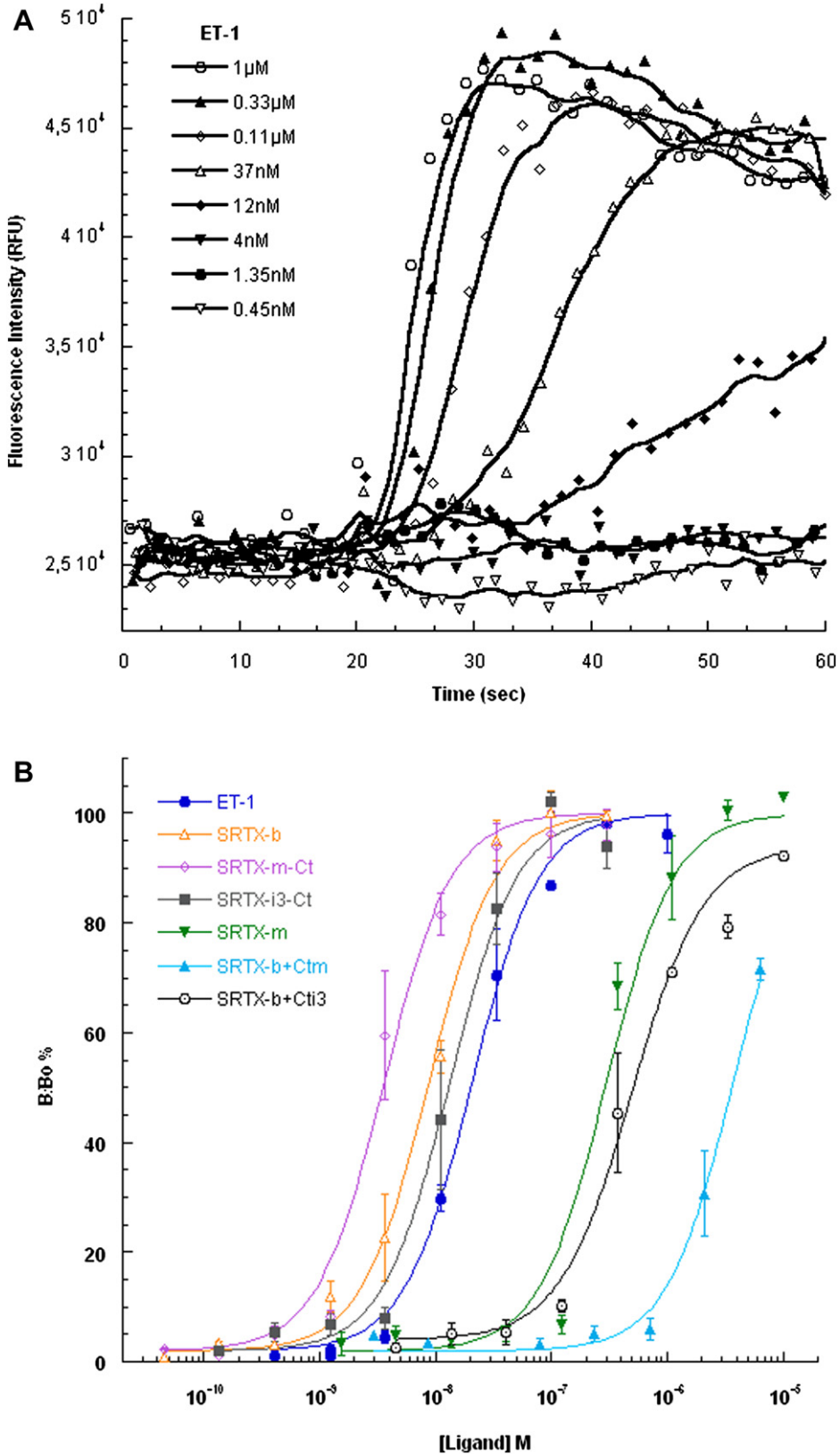

Fig. 5. Functional properties of ET-1 and SRTXs. A. Signals acquired for calcium fluorescence, using the FlexStation calcium assay kit, after the addition at 20 s of increasing concentrations of ET-1 (0.45 nM to 1 µM) on CHO cells expressing the ET_B receptor. B. Dose–response activation curves on ET_B receptor for the different ligands studied.

Table 2
Agonist potency of ET-1, s-SRTX, l-SRTXs and modified toxins on ET_B receptor ($pEC_{50} = -\log EC_{50}$).

Ligands	pEC_{50}
ET-1	7.91 ± 0.07
SRTX-b	8.10 ± 0.11
SRTX-m	6.53 ± 0.04
SRTX-i3	n.d
SRTX-m-Ct	8.39 ± 0.09
SRTX-i3-Ct	7.95 ± 0.15
SRTX-b+Ctm	5.45 ± 0.07
SRTX-b+Cti3	6.30 ± 0.19

Finally and in addition to the role of the C-terminal extremity previously discussed, our results help to better understand the molecular origin of the high affinity and selectivity of ET and SRTX on their receptors. For example, a comparative analysis of the affinity and selectivity of the different ligands studied in this paper (Table 1) with their amino acid sequences (Fig. 1), allows to precisely complete our knowledge on these interactions. To perform this analysis without taking into account the role of the C-terminal extension, sequence/affinity comparisons will be made on all the 21 amino acids ligands including natural (ET-1, ET-3, SRTX-b, SRTX-c) or truncated peptides (SRTX-m-Ct, SRTC-i3-Ct). Contribution of several positions in the CSH domain of the ligands appears critical for their affinity/selectivity profiles and agonist potency. Thus, at position +4 and +5, the presence of two Ser residues in ET-1 is associated with a lack of selectivity between both receptor subtypes while their substitution by a Lys–Asp (SRTX-b), a Phe–Thr (ET-3), an Asn–Asp (SRTX-m-Ct, SRTC-c), or a Thr–Asp (SRTX-i3-Ct) induces large and selective affinity decrease for ET_A receptor. As for the residue at position 9, previous studies have reported on the role of the positively charged side chain K9 that could be a major determinant of ET_A/ET_B ligand selectivity [25]. If this hypothesis may explain the five orders of magnitude decrease in selectivity observed for SRTX-i3-Ct or SRTX-c following the respective substitution of the Lys9 by a Leu or a Glu, the conservation of a positively charged residue at this position does not exclude a large and selective effect on ET_A interaction, as observed for the SRTX-b, the SRTX-m-Ct or the ET-3. Thus, if the presence of K9 in the peptide sequence seems always associated with a sub-nanomolar affinity for ET_B receptor, its substitution or charged-inversion is not a prerequisite to affect drastically and selectively the ET_A affinity (Fig. 1, Table 1). These results confirm the major role of the N-terminal and bend part of the peptide ligands in their selectivity of interaction with both receptor subtypes, as previously demonstrated by the high ET_B selectivity of peptide deleted of their N-terminal part [28]. Comparison of the primary sequences of l-SRTXs *versus* s-SRTXs and ETs reveals also differences at positions 12 and 13. Positions 12, 13 and 14 located within the conserved alpha-helix region, constitute an hydrophobic epitope in ET-receptors ligands involved in their high affinity binding. Indeed, alanine replacements of V12, Y13 and F14 result in a strong loss of ET-1 affinity [19]. Thus, it is proposed that the side chains at these positions are optimally oriented to interact with aromatic and hydrophobic residues of ET-receptors formed by the extracellular loops 1 and 2 together with the TM domains 2 and 3 [25]. Consequently, natural variations occurring in that region of ET-receptor ligands are often conservative in nature. In our case, SRTX-m-Ct and SRTX-i3-Ct display the unusual sequences M12-Y13-F14 and M12-N13-F14, suggesting that the presence of a methionine at position 12 associated or not with an asparagine at position 13 could be related with the important loss of affinity observed on ET_A receptor. Therefore, we hypothesize that the selectivity of peptide ligands for ET-receptors is supported by a multi-points attachment between residues in the CSH domain of the ligand and the extracellular domains or top of the TM domains of the receptors.

To conclude, our study analyzes for the first time the precise pharmacological profiles of short and long-SRTXs on cloned ET-receptors, demonstrates the critical role of the C-terminal extension in the very low affinity of l-SRTX for both ET-receptor subtypes and highlights the significant loss of the agonist potency associated with these additional residues. Nevertheless, these observations could not explain the persistent high toxicity observed for this new class of SRTXs and thus pave the way for several hypotheses. First, one explanation could be an endogenous maturation of l-SRTXs by specific endoproteases of the prey, liberating s-SRTXs. This assumption is particularly plausible for SRTX-i3 that possesses the same residues after the W21 than Big-ET-1 (V22-N23). However, preliminary *in vitro* experiments studying the effect of ECE and NEP on the processing of the two l-SRTX do not show any significant proteolytic cleavages of SRTX-m and SRTX-i3 (data not shown). Nevertheless, the enzymes tested *in vitro* may not correspond to those present *in vivo*. Another explanation could be the involvement *in vivo* of "atypical" ET-receptors, such as a new subtype which has been postulated in several papers [29,30] or involving an hetero-oligomerization, process that is known to modulate the pharmacological property of interacting ligands [31]. l-SRTXs could then interact more efficiently *in vivo* with these hetero-dimeric receptors as those studied in *in vitro* binding experiments. Finally, one of the most likely explanations is related to the fact that the agonist potency of the l-SRTX on the ET-receptors, at the origin of their lethal effect, may appear even if the toxin does not occupied all the receptor sites. Indeed, the agonist effect is largely amplified throughout the signalisation cascade explaining that the physiological effect could be observed at concentration lower than the Kd of the ligand. This hypothesis is reinforced by the agonist potency reported for the SRTX-m, which is only 40-fold lower than the SRTX-b, while affinity of SRTX-m is 4-orders of magnitude lower than that of SRTX-b. All these hypotheses should be evaluated properly in the near future giving special attention to the precise examination of the cardio-vascular effects of s-SRTXs and l-SRTXs *in vivo*.

Acknowledgements

We are grateful to a) Dr. Sabrina Corrazza (AxxamSpA, Milan, Italy) for providing CHO cells stably expressing the human ET_A receptors, and b) Drs Fatima Dkhissi and Anne Wijkuisen for providing CHO cells stably expressing the human ET_B receptors.

Appendix. Supplementary data

Supplementary data associated with this article can be found, in the online version, at doi:10.1016/j.biochi.2011.08.014.

References

[1] M. Sokolovsky, Endothelins and sarafotoxins: physiological regulation, receptor subtypes and transmembrane signaling, Trends Biochem. Sci. 16 (1991) 261–264.
[2] R.M. Kedzierski, M. Yanagisawa, Endothelin system: the double-edged sword in health and disease, Annu. Rev. Pharmacol. Toxicol. 41 (2001) 851–876.
[3] F. Ducancel, The sarafotoxins, Toxicon 40 (2002) 1541–1545.
[4] H. Tamaoki, Y. Kyogoku, K. Nakajima, S. Sakakibara, M. Hayashi, Y. Kobayashi, Conformational study of endothelins and sarafotoxins with the cystine-stabilized helical motif by means of CD spectra, Biopolymers 32 (1992) 353–357.
[5] A.R. Atkins, R.C. Martin, R. Smith, ^{1}H NMR studies of sarafotoxin SRTb, a nonselective endothelin receptor agonist, and IRL 1620, an ETB receptor-specific agonist, Biochemistry 34 (1995) 2026–2033.

[6] H. Kitamura, P. Cui, S. Sharmin, M. Yano, H. Kido, Binding of a new bioactive 31-amino-acid endothelin-1 to an endothelin ET(B) or ET(B)-like receptor in porcine lungs, Eur. J. Pharmacol. 465 (2003) 31–38.
[7] M.A. Hayashi, C. Ligny-Lemaire, Z. Wollberg, M. Wery, A. Galat, T. Ogawa, B.H. Muller, H. Lamthanh, Y. Doljansky, A. Bdolah, R. Stocklin, F. Ducancel, Long-sarafotoxins: characterization of a new family of endothelin-like peptides, Peptides 25 (2004) 1243–1251.
[8] L. Quinton, J.P. Le Caer, G. Phan, C. Ligny-Lemaire, J. Bourdais-Jomaron, F. Ducancel, J. Chamot-Rooke, Characterization of toxins within crude venoms by combined use of Fourier transform mass spectrometry and cloning, Anal. Chem. 77 (2005) 6630–6639.
[9] F. Ducancel, Endothelin-like peptides, Cell Mol. Life Sci. 62 (2005) 2828–2839.
[10] G. Mourier, S. Dutertre, C. Fruchart-Gaillard, A. Menez, D. Servent, Chemical synthesis of MT1 and MT7 muscarinic toxins: critical role of Arg-34 in their interaction with M1 muscarinic receptor, Mol. Pharmacol. 63 (2003) 26–35.
[11] F. Cordier, E. Vinolo, M. Veron, M. Delepierre, F. Agou, Solution structure of NEMO zinc finger and impact of an anhidrotic ectodermal dysplasia with immunodeficiency-related point mutation, J. Mol. Biol. 377 (2008) 1419–1432.
[12] K. Wüthrich, NMR of Proteins and Nucleic Acids New York (1986).
[13] J.P. Linge, M.A. Williams, C.A. Spronk, A.M. Bonvin, M. Nilges, Refinement of protein structures in explicit solvent, Proteins 50 (2003) 496–506.
[14] A.T. Brunger, P.D. Adams, G.M. Clore, W.L. DeLano, P. Gros, R.W. Grosse-Kunstleve, J.S. Jiang, J. Kuszewski, M. Nilges, N.S. Pannu, R.J. Read, L.M. Rice, T. Simonson, G.L. Warren, Crystallography & NMR system: a new software suite for macromolecular structure determination, Acta Crystallogr. D Biol. Crystallogr. 54 (1998) 905–921.
[15] R.A. Laskowski, D.S. Moss, J.M. Thornton, Main-chain bond lengths and bond angles in protein structures, J. Mol. Biol. 231 (1993) 1049–1067.
[16] Y. Cheng, W.H. Prusoff, Relationship between the inhibition constant (K1) and the concentration of inhibitor which causes 50 per cent inhibition (I50) of an enzymatic reaction, Biochem. Pharmacol. 22 (1973) 3099–3108.
[17] Y. Masuda, T. Sugo, T. Kikuchi, A. Kawata, M. Satoh, Y. Fujisawa, Y. Itoh, M. Wakimasu, T. Ohtaki, Receptor binding and antagonist properties of a novel endothelin receptor antagonist, TAK-044 [cyclo[D-alpha-aspartyl-3-[(4-phenylpiperazin-1-yl) carbonyl]-L-alanyl-L-alpha-aspartyl-D-2-(2-thienyl) glycyl-L-leucyl-D-tryptophyl]disodium salt], in human endothelinA and endothelinB receptors, J. Pharmacol. Exp. Ther. 279 (1996) 675–685.
[18] R. Bennes, B. Calas, P.E. Chabrier, J. Demaille, F. Heitz, Evidence for aggregation of endothelin 1 in water, FEBS Lett. 276 (1990) 21–24.
[19] J.P. Tam, W. Liu, J.W. Zhang, M. Galantino, F. Bertolero, C. Cristiani, F. Vaghi, R. de Castiglione, Alanine scan of endothelin: importance of aromatic residues, Peptides 15 (1994) 703–708.
[20] H. Tamaoki, R. Miura, M. Kusunoki, Y. Kyogoku, Y. Kobayashi, L. Moroder, Folding motifs induced and stabilized by distinct cystine frameworks, Protein Eng. 11 (1998) 649–659.
[21] E. Kochva, A. Bdolah, Z. Wollberg, Sarafotoxins and endothelins: evolution, structure and function, Toxicon 31 (1993) 541–568.
[22] H. Takashima, N. Mimura, T. Ohkubo, T. Yoshida, H. Tamaoki, Y. Kobayashi, Distributed computing and NMR constraint-based high-resolution structure determination: applied for bioactive peptide endothelin-1 to determine C-terminal folding, J. Am. Chem. Soc. 126 (2004) 4504–4505.
[23] S. Kimura, Y. Kasuya, T. Sawamura, O. Shinmi, Y. Sugita, M. Yanagisawa, K. Goto, T. Masaki, Structure-activity relationships of endothelin: importance of the C-terminal moiety, Biochem. Biophys. Res. Commun. 156 (1988) 1182–1186.
[24] M.A. Forget, N. Lebel, P. Sirois, Y. Boulanger, A. Fournier, Biological and molecular analyses of structurally reduced analogues of endothelin-1, Mol. Pharmacol. 49 (1996) 1071–1079.
[25] J. Lattig, A. Oksche, M. Beyermann, W. Rosenthal, G. Krause, Structural determinants for selective recognition of peptide ligands for endothelin receptor subtypes ETA and ETB, J. Pept. Sci. 15 (2009) 479–491.
[26] M. Macchia, S. Barontini, F. Ceccarelli, C. Galoppini, L. Giusti, M. Hamdan, A. Lucacchini, A. Martinelli, E. Menchini, M.R. Mazzoni, R.P. Revoltella, F. Romagnoli, P. Rovero, Toward the rational development of peptidomimetic analogs of the C-terminal endothelin hexapeptide: development of a theoretical model, Farmaco 53 (1998) 545–556.
[27] A. Ergul, R.L. Tackett, D. Puett, Identification of receptor binding and activation sites in endothelin-1 by use of site-directed mutagenesis, Circ. Res. 77 (1995) 1087–1094.
[28] R. Katahira, I. Umemura, M. Takai, K. Oda, T. Okada, A.Y. Nosaka, Structural studies on endothelin receptor subtype B specific agonist IRL 1620 [suc-[Glu9, Ala11,15]ET-1(8-21)] and its analogs with dipalmitoyl phosphatidylcholine vesicles by NMR spectroscopy, J. Pept. Res. 51 (1998) 155–164.
[29] O. Valdenaire, T. Giller, V. Breu, A. Ardati, A. Schweizer, J.G. Richards, A new family of orphan G protein-coupled receptors predominantly expressed in the brain, FEBS Lett. 424 (1998) 193–196.
[30] Z. Zeng, K. Su, H. Kyaw, Y. Li, A novel endothelin receptor type-B-like gene enriched in the brain, Biochem. Biophys. Res. Commun. 233 (1997) 559–567.
[31] N. Harada, A. Himeno, K. Shigematsu, K. Sumikawa, M. Niwa, Endothelin-1 binding to endothelin receptors in the rat anterior pituitary gland: possible formation of an ETA-ETB receptor heterodimer, Cell Mol. Neurobiol. 22 (2002) 207–226.
[32] P.M. Rose, S.R. Krystek Jr., P.S. Patel, E.C. Liu, J.S. Lynch, D.A. Lach, S.M. Fisher, M.L. Webb, Aspartate mutation distinguishes ETA but not ETB receptor subtype-selective ligand binding while abolishing phospholipase C activation in both receptors, FEBS Lett. 361 (1995) 243–249.
[33] S.R. Krystek Jr., P.S. Patel, P.M. Rose, S.M. Fisher, B.K. Kienzle, D.A. Lach, E.C. Liu, J.S. Lynch, J. Novotny, M.L. Webb, Mutation of peptide binding site in transmembrane region of a G protein-coupled receptor accounts for endothelin receptor subtype selectivity, J. Biol. Chem. 269 (1994) 12383–12386.